Article:
Barzadd, M.M., Lundqvist, M., Harris, C. et al. (11 more authors) (2022) Autophagy and intracellular product degradation genes identified by systems biology analysis reduce aggregation of bispecific antibody in CHO cells. New Biotechnology, 68. pp. 68-76. ISSN 1871-6784

https://doi.org/10.1016/j.nbt.2022.01.010

New BIOTECHNOLOGY 68 (2022) 68–76

Contents lists available at ScienceDirect

New BIOTECHNOLOGY

journal homepage: www.elsevier.com/locate/nbt

Autophagy and intracellular product degradation genes identified by systems biology analysis reduce aggregation of bispecific antibody in CHO cells

Mona Moradi Barzadd [a], Magnus Lundqvist [a], Claire Harris [c], Magdalena Malm [a], Anna-Luisa Volk [a], Niklas Thalén [a], Veronique Chotteau [b], Luigi Grassi [c], Andrew Smith [c], Marina Leal Abadi [c], Giulia Lambiase [d], Suzanne Gibson [c], Diane Hatton [c], Johan Rockberg [a,*]

[a] KTH - Royal Institute of Technology, School of Engineering Sciences in Chemistry, Biotechnology, and Health, Dept. of Protein Science, SE-106 91 Stockholm, Sweden
[b] KTH - Royal Institute of Technology, School of Engineering Sciences in Chemistry, Biotechnology, and Health, Dept. of Industrial Biotechnology, SE-106 91 Stockholm, Sweden
[c] Cell Culture & Fermentation Sciences, BioPharmaceutical Development, BioPharmaceuticals R&D, AstraZeneca, Cambridge, UK
[d] Analytical Sciences, BioPharmaceutical Development, BioPharmaceuticals R&D, AstraZeneca, Cambridge, UK and Advanced Biomanufacturing Centre, Department of Chemical and Biological Engineering, University of Sheffield, Mappin Street, Sheffield, UK

ARTICLE INFO

Keywords:
CHO cells
Aggregation
Autophagy
ER stress
Bispecific antibody
System biology

ABSTRACT

Aggregation of therapeutic bispecific antibodies negatively affects the yield, shelf-life, efficacy and safety of these products. Pairs of stable Chinese hamster ovary (CHO) cell lines produced two difficult-to-express bispecific antibodies with different levels of aggregated product (10–75% aggregate) in a miniaturised bioreactor system. Here, transcriptome analysis was used to interpret the biological causes for the aggregation and to identify strategies to improve product yield and quality. Differential expression- and gene set analysis revealed upregulated proteasomal degradation, unfolded protein response and autophagy processes to be correlated with reduced protein aggregation. Fourteen candidate genes with the potential to reduce aggregation were co-expressed in the stable clones for validation. Of these, HSP90B1, DDIT3, AKT1S1, and ATG16L1, were found to significantly lower aggregation in the stable producers and two (HSP90B1 and DNAJC3) increased titres of the anti-HER2 monoclonal antibody trastuzumab by 50% during transient expression. It is suggested that this approach could be of general use for defining aggregation bottlenecks in CHO cells.

Introduction

Mammalian cell lines have become the dominant expression system for therapeutic proteins and are currently used to manufacture more than 80% of all biopharmaceuticals approved on the market [1]. Monoclonal antibodies (mAbs) are used in treating a wide variety of diseases including cancer and autoimmune disorders [2]. Over the last decade, the biopharmaceutical industry has shifted its focus towards research and development of bispecific antibodies (BsAbs) due to their ability to bind two different epitopes at the same time, resulting in improved efficacy [3]. There are several different categories and formats of BsAbs, including IgG-like formats such as quadromas, knobs-into-holes, DuetMabs, and dual-variable domain immunoglobulins, which are created by combining the variable domains from two mAbs resulting in a dual-specific IgG-like molecule [3,4]. Despite all their advantages in biological activity, the production of BsAbs can be challenging as a result of their increased molecular complexity. For instance, one such challenge is to obtain the correct pairing and assembly of the heavy and light chains in order to generate two different sites for epitope binding [3,5]. This inherent structural complexity exposes BsAbs to product degradation events, with aggregation being one of the critical quality attributes which may halt new therapeutic

Abbreviation: BsAbs, bispecific antibodies; MSX, methionine sulfoximine; TPM, transcripts per million; VCD, viable cell density; ERAD, endoplasmic reticulum associated protein degradation; UPR, unfolded protein response; GRPs, glucose-regulated proteins.

* Corresponding authors at: KTH - Royal Institute of Technology, School of Engineering Sciences in Chemistry, Biotechnology, and Health, Dept. of Protein Science, SE-106 91 Stockholm, Sweden
E-mail address: johan.rockberg@biotech.kth.se (J. Rockberg).

https://doi.org/10.1016/j.nbt.2022.01.010
Received 16 August 2021; Received in revised form 31 January 2022; Accepted 31 January 2022
Available online 2 February 2022

candidates from proceeding to preclinical stages [3,6].

Aggregation can occur at multiple stages, from production to storage and administration of the therapeutic protein. The formation of protein aggregates is a major concern during drug development due to its negative impact on product yield, quality, safety and efficacy [7]. Several factors can influence the tendency of a protein to aggregate, including its primary-, secondary- and tertiary-structures, as well as glycosylation pattern and susceptibility to chemical damage. Moreover, cellular stress events associated with the expression of protein levels that surpass the folding- and secretion capacity of the cells have been reported to induce aggregation [7–9]. Along these lines, the imbalance of expression between antibody heavy chain (HC) and light chain (LC) is known to affect yield and aggregation [10,11]. Among the numerous strategies applied to reduce BsAb aggregation are the removal of aggregation-prone regions in the primary structure, improved bioprocessing conditions, media- and storage formulations as well as purification methodologies [7]. Various genetic engineering strategies have also been investigated to prevent intracellularly-formed aggregates and to improve protein secretion [12]. Some examples include the overexpression of endoplasmic reticulum (ER) chaperones, vesicle transporters, genes involved in the unfolded protein response (UPR) and signal recognition particles along with advances in signal peptide engineering and the introduction of regulatory elements to fine-tune the ratio between the HC and the LC [10,12].

Unfortunately, successful cell engineering solutions are not necessarily applicable to all host cell lines and expressed therapeutics. Many positive results have not been reproducible in settings differing from those where the original finding was elucidated [13,14]. This may be the result of the large number of genes investigated as well as the complex interactions that make up the protein production machinery of a cell. Additionally, the burden of constantly boosting expression titres is likely to have ramifications for many biological processes throughout the cell. Omics analysis has already helped to improve media optimisation and the identification of targets for genetic engineering [15,16]. The application of omics technologies also has the potential to strengthen understanding of the secretory machinery and the biological implications of producing high levels of recombinant proteins, which may in turn guide bioprocess optimisation and cell engineering strategies [15,17].

In this study, transcriptomic analysis was performed on stable CHO clones and pools producing two difficult-to-express and aggregation-prone BsAbs, in order to define cellular processes linked to both product aggregation and yield. Guided by differential gene expression and gene set analysis, four genes (HSP90B1, DDIT3, AKT1S1 and ATG16L1) were identified that significantly reduced the level of aggregated BsAb products when overexpressed and two (HSP90B1 and DNAJC3) that increased the titre of the anti-HER2 mAb trastuzumab in transiently transfected CHO cells. This study also highlights and discusses the importance of cellular homeostasis, finding the right level of transcription of heavy and light chains, and the observed biological differences between the cell lines, such as upregulation of genes involved in ER stress and autophagy.

Material and methods

Model CHO cell cultures

Ab1 and Ab2 are human bispecific antibodies with variable sequences generated by phage display and immunisation of mice. Stable transfectant pools (Ab2-less and Ab2-OPT-agg) and clonal cell lines (Ab1-less and Ab1-agg) were generated by nucleofection (Lonza, Basel, Switzerland) of the corresponding bispecific expression plasmid into the AstraZeneca (AZ, Cambridge, UK) proprietary CHO host, CAT-S, a derivative of CHO-K1 cells [18] and subsequent selection with methionine sulfoximine (MSX). Clonal cell lines were isolated by single cell cloning using fluorescence-activated cell sorting (FACS). Cells were routinely cultured in CD-CHO medium (ThermoFisher Scientific, Waltham, MA, USA) with 50 μM MSX in Erlenmeyer flasks at 140 rpm, 37 °C, 6% CO_2 and 70% humidity. Host cells were maintained in CD-CHO with 6 mM L-glutamine. All cell lines were adapted to AZ proprietary production medium before fed-batch culture.

Fed-batch culture and preparation of RNA samples

Fed-batch culture was performed in an ambr15 (Sartorius Stedim, Göttingen, Germany) using AZ proprietary, animal component free, production medium and feeds, in a 14-day process. Each cell line was assessed in quadruplicate vessels. Cells were maintained with 50% dissolved O_2, at 35.5 °C, and controlled pH. Glucose concentration was maintained during the fed-batch culture and measured daily with a glucose/lactate analyser (YSI Inc., Yellow Springs, USA). Samples for transcriptomic analysis were taken on day 8, taking triplicate samples from vessels with the highest viability. Aliquots of 5×10^6 cells were centrifuged at 300 *g* for 5 min, the supernatant removed and the pellet snap frozen on dry ice and stored at − 80 °C. Cells were then resuspended in 200 μL RNAlater (ThermoFisher Scientific, Waltham, MA, USA), samples were placed at 4 °C overnight and then stored at − 80 °C. Samples were thawed and RNA was extracted according to manufacturer's instructions with the Qiagen RNeasy® Plus Universal Mini Kit (Qiagen, Hilden, Germany). RNA integrity was checked with an Agilent RNA 6000 Nano kit (Agilent Technologies, Santa Clara, CA, USA) on an Agilent Bioanalyzer 2100 and samples with an RNA integrity number (RIN) > 8 were sent for subsequent sequencing on an Illumina platform at paired-end 2×150bp (Illumina HiSeq platform via a commercial service at GATC Biotech, Constance, Germany).

Titre assessment

Sample quantitation was performed using an Agilent 1260 high performance liquid chromatography (HPLC) system equipped with a binary pump (Agilent Technologies). A POROS™ A 20 affinity column of 2.1 mm × 30 mm, 0.1 mL (Thermo Fisher Scientific, Waltham, MA, USA) was employed using two mobile phases; buffer A: 10 mM sodium phosphate, 150 mM sodium chloride pH 7.2 (used for sample loading and washing of unbound impurities) and buffer B: 12 mM HCl / 150 mM sodium chloride pH 2.0 (used for protein elution step). The calibration curve was prepared using a corresponding reference material of known concentration. The run was carried out at 2 mL/min and the protein elution was monitored by A280 nm. Sample concentration was determined by integration of the eluted peak and plotting the peak area against the calibration curve.

Aggregation assessment by 2D-ProA – Size Exclusion Chromatography (SEC)

The first dimension Protein A method followed the same parameters as the mAb titre method described above but with an optimised elution (buffer B) at pH 3.0. Utilising 2D-LC Acquisition Software OpenLAB CDS, a single heart cut was diverted post first dimension detector via a 2D-LC valve. This material was stored in a loop capillary before being diverted into the second-dimension flow path. Aggregate analysis was performed via SEC in the second dimension on an Agilent 1290 high performance liquid chromatography (HPLC) system equipped with a binary pump (Agilent Inc.). A 6 min isocratic elution at 0.4 mL/min was performed using a mobile phase of 0.1 M sodium phosphate dibasic anhydrous and 0.1 M sodium sulfate adjusted to pH 6.0. Data were collected at 280 nm using a diode-array detector.

Transcriptomics analysis

Gene expression was quantified from raw sequencing data using kallisto [19] cDNA for cricetulus_griseus_picr, Ensemble release 99 [20] as reference with the addition of the antibody sequences. Differential

expression analysis was carried out using DESeq2 [21] and the raw counts from kallisto, imported with tximport [22]. P-values were calculated with Wald tests and the Benjamini-Hochberg method was used for multiple testing correction. Gene set analysis was performed using Piano [23] with its default settings for its runGSA function, fold changes and padj values from DESeq2, and gene sets were downloaded from MSigDB [24,25]. The heatmaps using GO slims in Fig. 2I were based on the consensus score from gene set statistics calculations with mean, median, sum, Stouffer and tailStrength tests and were calculated with Piano's consensus Heatmap function. Gene sets with the lowest consensus score of one, in either the distinct up- or down direction for either of the two comparisons, were included in the figure. The KEGG [26–28] pathway map was coloured using Pathview [29], but colours were changed to make it more colour-blind friendly. RNA-seq raw data has been deposited at Sequence Read Archive (SRA) and has BioProject ID: PRJNA739051.

Co-expression experiments with the model system, anti-HER2 mAb trastuzumab

Cell culture and transfection

ExpiCHO™ cells (Thermo Fisher Scientific, Waltham, MA, USA) were routinely cultivated in ExpiCHO™ expression medium (Thermo Fisher Scientific, Waltham, MA, USA), passaged according to the manufacturer's instructions and incubated at 37 °C, 5% CO_2 in humidified air and 120 rpm. In total 150×10^6 ExpiCHO™ cells at a density of 6×10^6 cells/mL were transfected using the standard protocol as suggested by the manufacturer with a total of 20 μg trastuzumab plasmid DNA (pKTH17_trastuzumab, heavy and light chain synthesised using Invitrogen GeneArt Gene Synthesis - ThermoFisher, Waltham, MA, USA) per transfection. In order to boost the expression level of trastuzumab while avoiding excessive translational burden on the cells, a 1:10 ratio between the helper genes and trastuzumab was chosen. The cells were transfected with 20 μg of the trastuzumab expression construct and 2 μg of the helper genes. An empty vector (pKTH16_empty) was used as a negative control in place of the helper genes. All transfections were made in duplicate and were harvested at day 8 post-transfection.

IgG purification

The supernatants, which were harvested at day 8 posttransfection, were sterile filtered through a 45 μm filter followed by addition of 200 μL phenylmethylsulfonyl fluoride (protease inhibitor) and stored at 4 °C overnight. The expressed antibodies were purified by Protein A facilitated purification on an ÄktaSTART system (GE Healthcare, Chicago, IL, USA) using mAbSelectSuRe columns (GE Healthcare). A 20 mM sodium phosphate, 0.15 M sodium chloride (pH 7.3) buffer was used as binding and wash buffer, 0.1 M glycine (pH 2.5) as elution buffer and 1 M Tris–HCl (pH 8.5) as neutralisation buffer.

SEC of transient cultures

The purified trastuzumab was buffer exchanged into phosphate-buffered saline (PBS) using Amicon 3 kDa MWCO centrifugal filtration units (Merck Millipore, Kenilworth, NJ, USA) according to the manufacturer's recommendations prior to SEC analysis. In total, 20 μg IgG in 70 μL sample were injected onto a Superdex Increase 200 10/30 GL gel filtration column (GE Healthcare) coupled to an Agilent 1200 series HPLC system (Agilent Technologies, Santa Clara, CA, USA). SEC runs were performed at a 0.5 mL/min flow rate with PBS as a running buffer. Eluted protein fragments were detected by an online 280 nm absorption measurement.

Co-expression experiments with the bispecific antibodies

Cell culture and transfection

Ab-1-agg and Ab-2-OPT-agg cell lines were transfected using a nucleofector (Lonza, Basel, Switzerland) of 1×10^7 cells with 6 μg DNA and recovered into 2 mL proprietary production medium in a 24 deep well plate. Plates were incubated at 210 rpm, 37 °C, 6% CO_2 in a shaking incubator. Four hours post-transfection, proprietary feeds and glucose were added and the temperature was reduced to 34 °C. Cells were fed again at day 4 post-transfection. Titre was measured on day 6 post-transfection using the same methods described above. Viable cell density (VCD) and viability were measured using a plate-based method using trypan blue exclusion with imaging performed by a CellaVista (Synentec, Elmshorn, Germany).

Antibody purification and aggregation assessment

Bispecific mAb was purified from the harvested cell culture supernatant by Protein A affinity chromatography using 200 μL volume PhyTip® columns (PhyNexus Inc., San Jose, CA, USA) containing 20 μL of ProPlus (MabSelect SuRe™) affinity resin (PhyNexus Inc, San Jose, CA, USA) with a Tecan Freedom EVO® 200 robotic liquid handler (TECAN Group Ltd, Männedorf, Switzerland). A DropSense 96 (Unchained Labs, Ghent, Belgium) was used for measuring sample recovery post-purification. High-throughput aggregation analysis was by SEC and performed on an Agilent 1260 Infinity II UHPLC System equipped with a degasser, quaternary pump, thermostatted multisampler, and diode array detector. The method used an Aquity BEH SEC column (1.7 μm, 2.1 ×150 mm, 200 Å; Waters, Milford, USA) and a mobile phase composed of 50 mM sodium phosphate buffer, 200 mM sodium chloride, pH 6.8 eluted with a sub-4 min isocratic run at 0.15 mL/min. The column oven was set to 25 °C and the injection volume was 10 μL. Data analysis was achieved with Agilent OpenLAB CDS ChemStation Edition, version C.01.07.

Western blotting

Protein samples were generated using Radio Immuno Precipitation (RIPA) buffer supplemented with protease inhibitors (Thermo Fisher, Waltham, MA, USA) and separated by SDS-polyacrylamide gel electrophoresis (PAGE) using 3–8% Tris-acetate gels (Thermo Fisher, Waltham, MA, USA). Proteins were transferred to PVDF membranes using an iBlot (Thermo Fisher, Waltham, MA, USA) and blocked with Intercept blocking buffer (Li-Cor, Lincoln, NE, USA). Membranes were probed with antibodies against human IgG (Sigma, St. Louis, MO, USA. Catalogue number: SAB3701290) and GAPDH (RRID: AB_10977387, Thermo Fisher, Waltham, MA, USA). Detection was performed with 680RD or 800CW-conjugated secondary antibodies (Li-Cor, Lincoln, NE, USA. Catalogue numbers: 926–68070 and 926–32211) and blots imaged with a ChemiDoc MP (BioRad, Hercules, CA, USA). Aggregate levels were quantified by determining the band intensities using BioRad Image Lab software. The obtained values were normalised against band intensity of GAPDH.

Results

Cell lines expressing the same bispecific antibody produced different amounts of aggregated product

This study aimed to identify aggregation bottlenecks of two different BsAbs (Ab1 and Ab2) when stably expressed in CHO cells. Two high-producing clones, "Ab1-less" (Ab1 antibody with less aggregation) and "Ab1-agg" (Ab1 producer with more aggregation), engineered with the same Ab1 expression vector but displaying varying degrees of product aggregation, were selected for the Ab1 antibody. For Ab2, stable transfectant pools "Ab2-less" and "Ab2-OPT-agg" were generated, with the latter involving the use of a vector containing a codon-optimised HC (hence "OPT" in the name). The molecular structures of Ab1 and Ab2 were constructed respectively by fusing a single-chain variable fragment (scFv) with the CH3 region (Fig. 1A) and in the hinge region between the Fab and the Fc region (Fig. 1B), respectively. The properties of these bispecific formats have previously been described [30]. Both pairwise comparisons showed significant differences in titre, cell specific

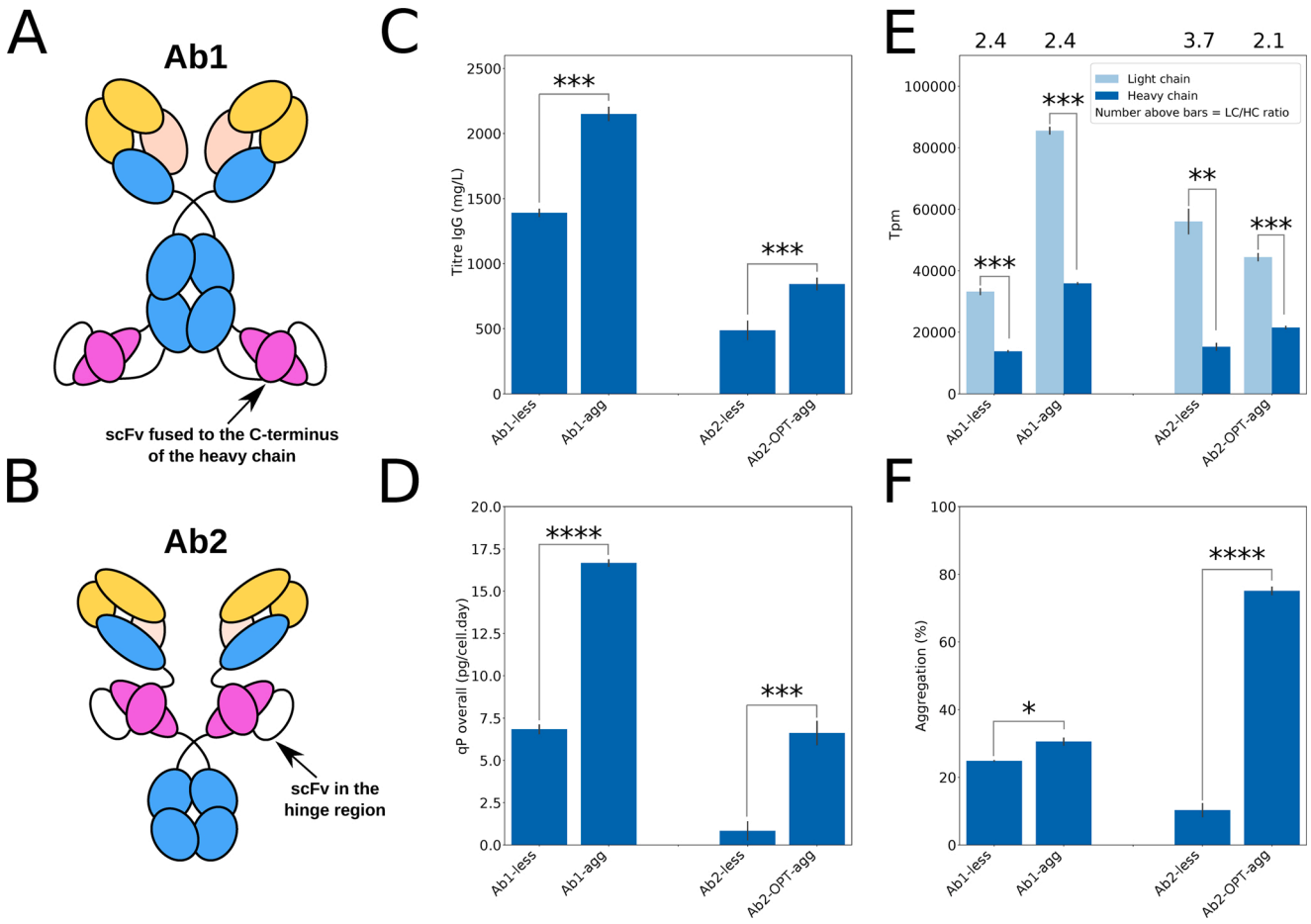

Fig. 1. Antibody schematics, cell-specific productivity and product aggregation from 14-day fed-batch cultures for two pairwise comparisons. Bars show mean values (n = 3), error bars, standard deviation (n = 3), and student's t-test, two-sample unequal variance was used to calculate significance (* ≤ p value 0.05, ** ≤ 0.01, *** ≤ 0.001, **** ≤ 0.000). A) Structural schematic of Ab1. Antibody colour code: yellow = variable region, blue = constant region, cerise = scFv (single-chain variable fragment) B) Structural schematic of Ab2. Additionally, Ab2-OPT-agg contained a codon-optimised heavy chain. C) IgG titre (mg/L) D) Cell specific productivity (qP) (pg/cell.day). E) RNA expression levels of light- and heavy chain (TPM), and light chain/heavy chain ratios. F) Proportion of aggregated antibody product (%).(For interpretation of the references to colour in this figure legend, the reader is referred to the web version of this article.)

productivity, and aggregation. Ab1-agg expressed more antibody mRNA and resulted in higher titre and cell specific productivity (qP) (2.1 g/L and 12.5 pg/cell.day) compared to Ab1-less (1.4 g/L and 5.1 pg/cell.day) (Fig. 1C-D). Ab1-agg expressed more than twice as much antibody mRNA compared to Ab1-less. The expression of Ab1 HC and LC corresponded to 35,000 transcripts per million (TPM) and 85,000 TPM, respectively, whereas Ab1-less expressed HC at 14,000 TPM and LC at 33,000 TPM (Fig. 1E) resulting in a LC:HC ratio of approximately 2.4 for both clones. Moreover, Ab1-agg showed a 5% increase in aggregation compared to Ab1-less (Fig. 1F). Ab2-OPT-agg produced a higher titre and qP than Ab2-less (0.85 g/L and 6.6 pg/cell.day compared to 0.45 g/L and 0.8 pg/cell.day, Fig. 1C-D), while the LC:HC expression ratio was considerably shifted when comparing Ab2-less and Ab2-OPT-agg, with 3.7 for Ab2-less and 2.1 for Ab2-OPT-agg (Fig. 1E). The alteration in LC:HC ratio, combined with an expected higher translation efficiency due to the codon optimisation, led to a higher amount of HC protein in Ab2-OPT-agg. Interestingly, the antibody aggregation level for Ab2-OPT-agg was significantly higher than clone Ab2-less (75% vs. 10%, respectively) (Fig. 1F).

Early cell death and rapid accumulation of lactate as distinguishing traits of Ab2-less cells

Viable cell density (VCD), viability, glucose and lactate levels were measured throughout the fed-batch culture (Fig. 2A-H). Ab1-less showed a faster growth rate than Ab1-agg with maximum VCD achieved on day 7 rather than day 10, reaching 29.3 × 10^6 cells/mL and 15.5 × 10^6 cells/mL, respectively (Fig. 2A). No significant difference was observed in viability, but there was a small but significant difference in lactate levels between days 7 and 11, with Ab1-less reaching up to 1.4 g/L higher lactate concentration (Fig. 2B-C). Glucose concentration was maintained during the fed-batch culture and was observed to remain steady for both clones throughout the experiment (Fig. 2D). Ab2-less and Ab2-OPT-agg showed a larger difference in regard to VCD, viability and lactate concentration than the Ab1 clones. On day 5, the VCD and viability had begun to drop for Ab2-less (Fig. 2E-F). As was also seen for the Ab1 clones, the glucose concentration was similar for both Ab2 clones up until the final days of cultivation (Fig. 2H). The lactate concentration on day 2 was higher in Ab2-less and continued to increase steadily until the end of the fed-batch culture (Fig. 2G).

The differences observed in cell death, growth and division were also supported by the transcriptomic data. In Ab2-less cells, genes enriched in the cell death pathway were significantly upregulated, while genes enriched in the chromosome segregation process were significantly downregulated. (Fig. 2I, Supplementary GSA results). Moreover, Ab2-less appeared to undergo a cellular transformation possibly associated with cell death, since upregulation of cell differentiation and membrane organization were observed. With considerably more GOSlim terms presenting a significant change, the difference between Ab2-less and Ab2-OPT-agg was much greater than between the two Ab1 clones

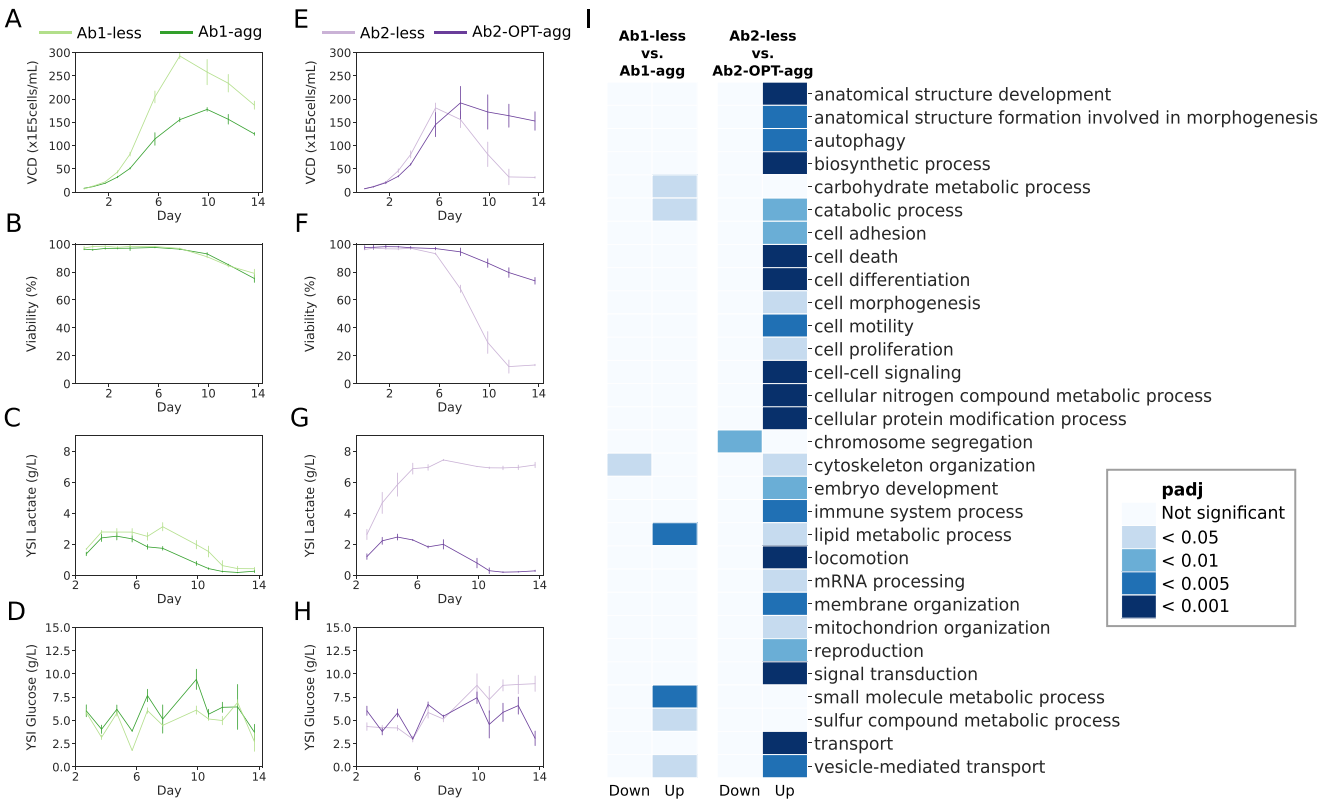

Fig. 2. Viable cell density (VCD), viability, lactate and glucose concentration from 14-day fed-batch cultures and gene set analysis with GOSlims for the two comparisons. Lines show mean values (n = 3), error bars represent the standard deviation, and student's t-test, two-sample unequal variance was used to calculate significance (p-value < 0.01 was considered significant). A) Viable cell density (VCD) for Ab1. B) Viability (%) for Ab1 C) Lactate (g/L) for Ab1 D) Glucose (g/L) for Ab1 E) Viable cell density (VCD) for Ab2. F) Viability (%) for Ab2 G) Lactate (g/L) for Ab2 H) Glucose (g/L) for Ab2. I) Gene set analysis with GO slims displaying high-level cellular processes that were significantly (padj < 0.05) up- or downregulated for either of the two comparisons.

(Fig. 2I, Supplementary GSA results). The increased lactate production in Ab2-less may in part be explained by the upregulation of glucose catabolic processes (Supplementary GSA results), and the higher expression (padj < 0.01) compared to Ab2-OPT-agg for several glycolysis genes (Supplementary DE results). Among these genes, ENO2, HK2, PFKFB3 and PFKFB4 showed the highest degree of upregulation (>0.5 $\log_2$ fold change).

Ab1-agg clone primarily demonstrated an upregulated ER stress and unfolded protein response (UPR) compared to Ab1-less

Although clones Ab1-less and Ab1-agg produced the same antibody protein sequence, Ab1-agg produced more antibody mRNA resulting in a higher titre, albeit in a more aggregated form, as was seen in Fig. 1C-F. When comparing the gene expression of the two clones, the most upregulated gene sets (considering p-values) were associated with ER stress and the UPR in Ab1-agg (Fig. 3A, Supplementary GSA results). IRE1-mediated UPR, as well as responses to topologically incorrect protein, ER stress, and PERK-mediated UPR were among the most upregulated gene sets in Ab1-agg compared to Ab1-less. Other top upregulated gene sets involved related processes, such as protein stabilisation, retrograde protein transport from ER to cytosol, Golgi organization and vesicle transport. The most upregulated genes (considering fold change and padj < 0.01) related to ER stress and UPR cover a variety of functions. They serve as chaperones protecting polypeptides from misfolding upon translocation (HSPA5, HSP90B1, DNAJC3), inducing cell cycle arrest and apoptosis (DDIT3) and rearranging disulphide bonds (PDIA4). The remaining genes are part of endoplasmic reticulum associated protein degradation (ERAD) and the ubiquitin ligase complex (UBXN8, HERPUD1, DNAJB9) (Fig. 3B). These selected genes are likely to be crucial for cells to manage an elevated load of aggregation-prone antibody polypeptides in the ER, and were overexpressed transiently in Ab1-agg aiming to reduce aggregation (Fig. 3C). On average, both HSP90B1 and DDIT3 reduced aggregation from 27% to 23%. However, DDIT3 (as well as UBXN8, HSPA5, and HERPUD1) also led to a reduced titre (Fig. 3D). A western blot to detect intracellular levels of BsAb revealed that some of the higher molecular weight bands had decreased in intensity in samples with co-expression of helper genes (Supp. Fig. 1A). To further assess their impact on antibody production, these genes were co-expressed together with the anti-HER2 antibody trastuzumab. Only low amounts of aggregates were observed for the trastuzumab control, and this did not significantly change in the samples with co-expressed helper genes (Supp. Fig. 2). However, importantly, the lumenal chaperones, HSP90B1 and DNAJC3, did have a positive impact on protein expression, improving trastuzumab titre by 59% and 47%, respectively (Fig. 3E).

Ab2-less had upregulated genes related to autophagy and neurodegenerative diseases compared to Ab2-OPT-agg

The major difference between Ab1-less and Ab1-agg was the upregulation of ER-stress and UPR. However, none of the upregulated gene sets (Fig. 3A) showed a significant (padj < 0.01) up- or downregulation when comparing the two Ab2 producers (Supplementary GSA results). Nevertheless, the most upregulated ER stress genes in Ab1-agg compared to Ab1-less (Fig. 3B) were also upregulated in Ab2-OPT-agg compared to Ab2-less with one exception - DDIT3, a gene responsible for triggering cell cycle arrest and apoptosis (see Supplementary DE results). Notably, Ab2-less and Ab2-OPT-agg differed in the upregulation of autophagy and related processes, such as autophagosome organization, endosome organization, SNARE interactions in vesicular transport, and the lysosome (Supplementary GSA results). 127 of the

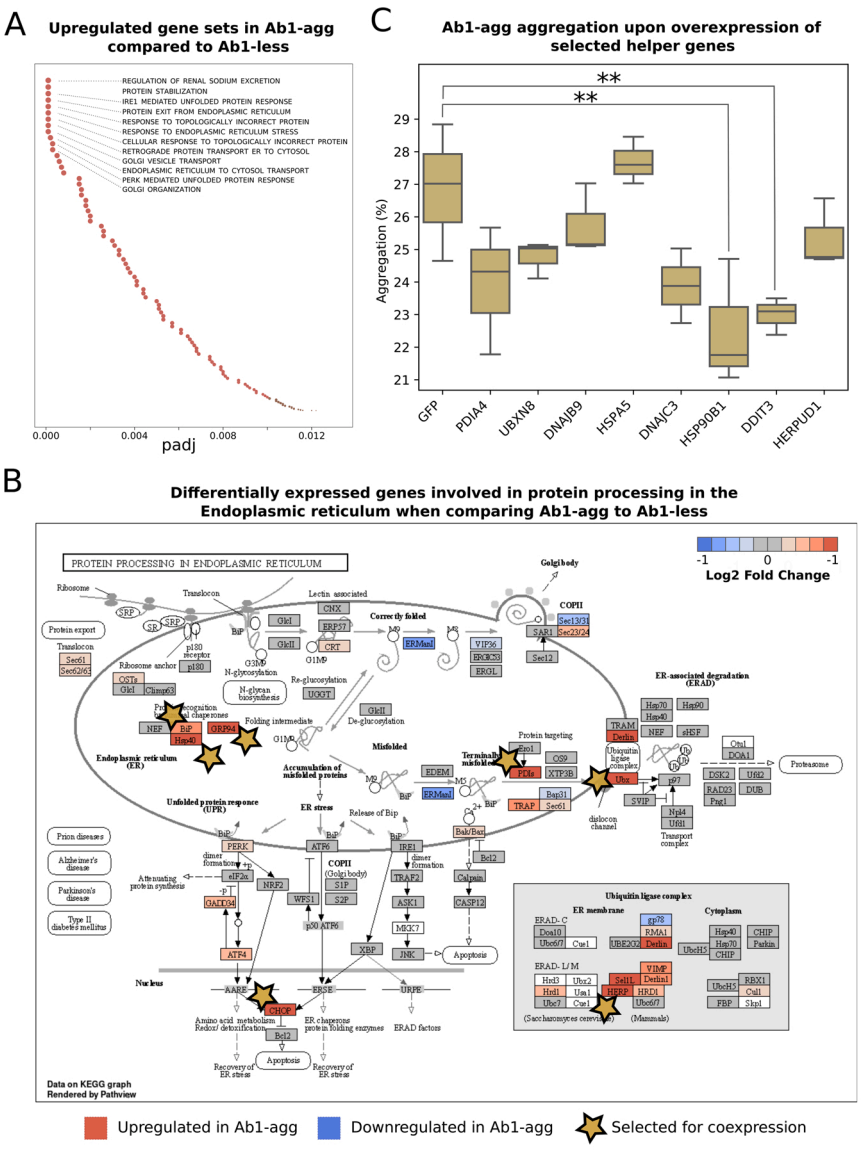

Fig. 3. ER-stress and overexpression of ER-stress genes in Ab1-agg. A) Gene set analysis showing the most significant and distinctly upregulated biological processes in Ab1-agg compared to Ab1-less. B) Differentially expressed genes involved in protein processing in the ER when comparing clone Ab1-agg to Ab1-less. The fold changes for genes that differed significantly in expression are visualised in red (upregulation) and blue (downregulation). Genes with the biggest upregulation in Ab1-agg were selected for overexpression and are marked with stars. C) Overexpression of selected ER-stress genes in Ab1-agg. Based on three replicates (n = 3) and Dunnett's multiple comparisons test with a control overexpressing GFP was used to calculate significance (** ≤ 0.01). D) Antibody titre for Ab1-agg upon overexpression of selected genes associated with ER-stress. Based on three replicates (n = 3) and Dunnett's multiple comparisons test with a control overexpressing GFP was used to calculate significance (** ≤ padj 0.01, **** ≤ 0.0001). E) Antibody titre upon co-expressing the selected genes associated with ER-stress together with trastuzumab (TRAZ). Dunnett's multiple comparisons test with TRAZ as control was used to calculate significance (** ≤ padj 0.01, *** ≤ 0.001).(For interpretation of the references to colour in this figure legend, the reader is referred to the web version of this article.)

421 genes populating all these sets were found to be significantly (padj < 0.01) upregulated and 67 downregulated in Ab2-less compared to Ab2-OPT-agg (Fig. 4A). Noticeable among these upregulated genes were AKT1S1, PIK3C3, ATG101, LAMP2, TOLLIP and ATG16Ll, which are involved in the degradation of cellular material by autophagy [31–33]. These genes were subsequently transiently expressed in Ab2-OPT-agg to evaluate whether their overexpression could reduce its aggregation (Fig. 4B). Here, both ATG16L1 and AKT1S1 significantly reduced aggregation from approximately 52% to 45%. LAMP2 was the only gene that significantly lowered the titre when overexpressed (Fig. 4C). For these helper genes, a western blot of the intracellular BsAb content showed a reduction of aggregation species when ATG16L1 and AKT1S1 were co-expressed, for which one of two aggregation bands was no longer detectable with the software (Supp. Fig. 1B). Other differences in biological processes between Ab2-less and Ab2-OPT-agg included the upregulation of various signalling pathways (JAK-STAT, MAPK, ERBB), for Ab2-less compared to Ab2-OPT-agg (Supplementary GSA results). Among them were some of the significantly upregulated genes that showed the biggest difference in expression (padj < 0.01, $\log_2$ fold change > 3), namely, IL19 (JAK-STAT), AREG (ERBB), PLA2G4E and FLNC (MAPK). Protein synthesis appeared to be downregulated in Ab2-less compared to Ab2-OPT-agg as genes involved in translation initiation and the ribosome were primarily found to be downregulated (Supplementary GSA results).

Discussion

In this study, by evaluating transcriptomic data from two stable CHO clones, as well as two stable pools, producing two different difficult-to-express human BsAbs (Ab1 and Ab2), the biosynthetic differences between cell lines with different antibody expression profiles are presented, particularly regarding processes closely associated with protein production and aggregation.

Ab1-agg expressed more than twice as much antibody mRNA compared to Ab1-less, possibly leading to increased ER-stress and the UPR. It has been reported that the overexpression of an antibody and the enhanced misfolded polypeptide chains in CHO cells correlate with a rise of both BiP (HSPA5) and CHOP (DDIT3) levels [34,35]. BiP binds to the Ig HC before its assembly with the LC. The overexpression and incomplete glycosylation of therapeutic proteins have been shown to increase the activity of BiP in the ER. Three ER-membrane bound sensors, PERK, ATF6 and IRE1 are associated with BiP. As a consequence of ER stress, BiP dissociates from these sensors and binds to the misfolded polypeptide, activating the UPR to restore ER homeostasis. First, the UPR tries to restore ER homeostasis by initiating mechanisms to both inhibit further protein synthesis and to increase the protein folding capacity. If this approach fails, due to excessive ER stress and high levels of misfolded proteins, the UPR activates genes such as DDIT3, which induces cell cycle arrest and promotes cell death via apoptosis [36]. BiP, DDIT3 and other ER-stress-related genes involved in IRE1- and PERK-mediated UPR, were upregulated in Ab1-agg. This suggests that the higher abundance of antibody mRNA impaired ER homeostasis, which would explain the reduction in cell growth in Ab1-agg. The use of weak promoters to drive BsAb gene expression may favour the reduction of aggregate levels in Ab1, however, this may come with a decline in expression titre. Alternatively, the upregulation of helper genes promoting protein folding may mitigate aggregation whilst maintaining desirable expression titres [9].

In Ab1-agg, the most upregulated genes considering fold change related to ER stress and UPR were HSPA5, HSP90B1, DNAJC3, DDIT3, PDIA4, UBXN8, HERPUD1 and DNAJB9. Hence, they were suspected to be crucial when the cell folding machinery was overwhelmed during antibody production and were evaluated as helper genes. Overexpression of HSP90B1 and DDIT3 in Ab1-agg reduced antibody aggregation significantly, although DDIT3 also lowered the titre. The reduction in titre is perhaps unsurprising as DDIT3 promotes cell death. However, it has previously been shown to increase recombinant protein production, hence its influence on titre appears to be context-dependent [34].

Co-expression experiments with the first three genes HSPA5, HSP90B1 and DNAJC3, which operate as lumenal chaperones that protect polypeptides from misfolding upon translocation, resulted in the highest titre increase compared to the other helper genes for trastuzumab. Here, a significant titre improvement of 59% and 47% was obtained for HSP90B1 and DNAJC3, respectively. As minimal levels of aggregates were observed, both for the trastuzumab control and upon helper gene co-expression, we believe this supports a more general applicability of these genes to improve antibody production. HSP90B1 (and HSPA5) are members of a family of glucose-regulated proteins (GRPs) found in the ER and which protect polypeptides from misfolding upon translocation [37]. DNAJC3 is a member of the DNAJ family, which is a lumenal ER protein. Upon its interaction with BiP, it selectively binds to misfolded polypeptides in the ER and is believed to be a pro-folding co-chaperone to BiP [38]. HSP90B1 has previously been tested in a co-expression study to improve the productivity of erythropoietin (EPO) in CHO cells, without showing any positive effect [14].

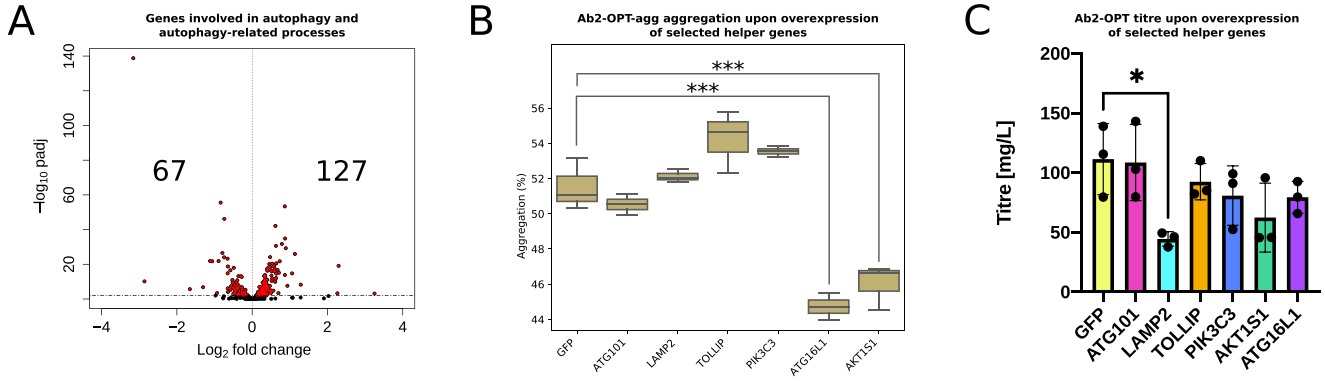

Fig. 4. Differences between Ab2-OPT-agg and Ab2-less and overexpression of selected autophagy genes in Ab2-OPT-agg. A) Differentially expressed genes involved in autophagy and autophagy-related gene sets (autophagosome organization, endosome organization, SNARE interactions in vesicular transport lysosome, and lysosome). Red dots represent genes with a significant change when comparing Ab2-OPT-agg to Ab2-less and black dots show genes with a non-significant difference. The numbers state the number of red dots on each side. Genes on the right-hand side were more expressed in Ab2-OPT-agg and genes on the left-hand side were more expressed in Ab2-less. B) Overexpression of selected autophagy genes in Ab2-OPT-agg. Based on three replicates (n = 3) and Dunnett's multiple comparisons test with a control overexpressing GFP was used to calculate significance (*** ≤ 0.001). C) Antibody titre for Ab2-OPT-agg upon overexpression of selected genes associated with autophagy. Based on three replicates (n = 3) and Dunnett's multiple comparisons test with a control overexpressing GFP was used to calculate significance (* ≤ padj 0.05).(For interpretation of the references to colour in this figure legend, the reader is referred to the web version of this article.)

Potentially, the effect on titre could be further enhanced if their expression was tuned to an optimal level or used in combination with other helper genes. It has also been suggested by different studies that overexpression of several ER-related chaperones or proteins might be necessary to significantly improve the productivity of recombinant proteins [34].

Compared to Ab2-OPT-agg, Ab2-less yielded a lower titre and a markedly less aggregated product, while decreasing in viability earlier in the fed-batch process, and genes associated with autophagy were upregulated. The higher mRNA expression for the HC, together with an expected increase in translation efficiency due to its codon optimisation, was assumed to be the cause of the high aggregation in Ab2-OPT-agg. It has been confirmed in previous studies that if the expression level of HC is too high, it can interfere with optimal expression of recombinant IgG in CHO cells [39]. In this scenario, the LC:HC ratio could be optimised by, for example, using different promoters or regulatory elements to either increase the amount of LC or decrease HC [10,40]. Other alternatives that could be applied to reduce aggregation include changing the hypothermic conditions [41], or switching to a perfusion process [42].

Upon incorrect folding in the ER, polypeptides may be targeted to different degradation paths to avoid the toxic effects of protein aggregates. The primary route of protein degradation is translocation of unfolded polypeptides into the cytosol for degradation by the proteasome. This non-lysosomal degradation machinery requires soluble single peptide species, while protein aggregates require degradation by autophagy [43]. In the latter process, protein aggregates can be bundled and enclosed by an autophagosome that is fused with a lysosome or a late endosome, where the aggregates are degraded. Ab2-less showed an upregulation of autophagy, autophagosome and endosome organization, lysosome, endosome to lysosome transport, and SNARE interactions in vesicular transport compared to Ab2-OPT-agg. Six autophagy-related genes that showed significantly higher expression in Ab2-less were overexpressed to see if they could improve the antibody production in Ab2-OPT-agg. Of these genes, both AKT1S1 and ATG16L1 significantly reduced aggregation. Again, the aggregation was only reduced by a small amount, but the impact of these genes could also potentially be further improved by fine-tuning their expression. AKT1S1 regulates mTORC1 activity, which controls autophagy among other biological processes [44] and ATG16L1 is involved in autophagosome formation [45]. The upregulation of autophagy in Ab2-less could be due to the lower viability in this culture, and not caused by protein aggregation. Another plausible explanation for the differences in aggregation levels and biological processes is that Ab2-less managed to re-translocate unfolded polypeptides to the cytosol, but the proteasome was overloaded, resulting in cytosolic aggregates that required autophagic degradation.

Conclusion

The aim of this study was to find strategies to improve yield and quality, and in particular to reduce antibody aggregation. To this end, HSP90B1, DNAJC3, AKT1S1, and ATG16L1 are presented as promising helper genes during recombinant antibody production. It has not previously been described that overexpression of any of these genes can have a positive effect on antibody production by reducing aggregation or improving titres. This study has also highlighted the importance of having a good level of antibody expression and balance between heavy and light chains; here, analogous producers with differences in antibody mRNA levels (Ab1) and the HC:LC ratio (Ab2) displayed significant differences in titre, aggregation and biological responses characterised by transcriptomic analysis. Consequently, finding a favourable balance in expression for difficult-to-express antibodies is of great importance in order to maintain a cellular balance for higher yield and quality as potential outcomes.

Declaration of Competing Interest

The authors declare the following financial interests/personal relationships which may be considered as potential competing interests: Claire Harris, Luigi Grassi, Suzanne Gibson, Andrew Smith and Diane Hatton are employees of AstraZeneca and may own stock or stock options. The other authors declare no financial or commercial conflict of interest.

Acknowledgements

The authors thank Lina Li, Jie Zhu and Soojin Han for the generation of the stable CHO clones and pools as well as Darren Geoghegan for support in performing the microbioreactor evaluation. This work was supported by the Knut and Alice Wallenberg Foundation, AstraZeneca, Swedish Foundation for Strategic Research (SSF), Swedish Innovation Agency Vinnova through AAVNova, GeneNova, CellNova and AdBIOPRO and the Novo Nordisk Foundation (grant no. NNF10CC1016517). Data handling was enabled by resources provided by the Swedish National Infrastructure for Computing (SNIC) at UPPMAX partially funded by the Swedish Research Council through grant agreement no. 2018-05973.

Author contributions

MMB and CH carried out the experiments with support from MM, ALV and NT. ML performed the transcriptomics analysis with support from LG. MMB and ML wrote the initial manuscript draft. All authors provided input on the research and/or the manuscript. DH and JR supervised the project.

Appendix A. Supporting information

Supplementary data associated with this article can be found in the online version at doi:10.1016/j.nbt.2022.01.010.

References

[1] Walsh G. Biopharmaceutical benchmarks 2018. Nat Biotechnol 2018;36:1136–45. https://doi.org/10.1038/nbt.4305.
[2] Castelli MS, McGonigle P, Hornby PJ. The pharmacology and therapeutic applications of monoclonal antibodies. Pharmacol Res Perspect 2019;7:e00535. https://doi.org/10.1002/prp2.535.
[3] Brinkmann U, Kontermann RE. The making of bispecific antibodies. MAbs 2017;9:182–212. https://doi.org/10.1080/19420862.2016.1268307.
[4] Fan G, Wang Z, Hao M, Li J. Bispecific antibodies and their applications. J Hematol Oncol 2015;8:130. https://doi.org/10.1186/s13045-015-0227-0.
[5] Wang Q, Chen Y, Park J, Liu X, Hu Y, Wang T, et al. Design and production of bispecific antibodies. Antibodies 2019;8:43. https://doi.org/10.3390/antib8030043.
[6] Gomez N, Lull J, Yang X, Wang Y, Zhang X, Wieczorek A, et al. Improving product quality and productivity of bispecific molecules through the application of continuous perfusion principles. Biotechnol Prog 2020;36:e2973. https://doi.org/10.1002/btpr.2973.
[7] Wang W, Roberts CJ. Protein aggregation – mechanisms, detection, and control. Int J Pharm 2018;550:251–68. https://doi.org/10.1016/j.ijpharm.2018.08.043.
[8] le Fourn V, Girod PA, Buceta M, Regamey A, Mermod N. CHO cell engineering to prevent polypeptide aggregation and improve therapeutic protein secretion. Metab Eng 2014;21:91–102. https://doi.org/10.1016/j.ymben.2012.12.003.
[9] Delic M, Göngrich R, Mattanovich D, Gasser B. Engineering of protein folding and secretion - strategies to overcome bottlenecks for efficient production of recombinant proteins. Antioxid Redox Signal 2014;21:414–37. https://doi.org/10.1089/ars.2014.5844.
[10] Eisenhut P, Mebrahtu A, Moradi Barzadd M, Thalén N, Klanert G, Weinguny M, et al. Systematic use of synthetic 5′-UTR RNA structures to tune protein translation improves yield and quality of complex proteins in mammalian cell factories. Nucleic Acids Res 2020;48(20):e119. https://doi.org/10.1093/nar/gkaa847.
[11] Ho SCL, Koh EYC, van Beers M, Mueller M, Wan C, Teo G, et al. Control of IgG LC:HC ratio in stably transfected CHO cells and study of the impact on expression, aggregation, glycosylation and conformational stability. J Biotechnol 2013;165:157–66. https://doi.org/10.1016/j.jbiotec.2013.03.019.
[12] Zhou Y, Raju R, Alves C, Gilbert A. Debottlenecking protein secretion and reducing protein aggregation in the cellular host. Curr Opin Biotechnol 2018;53:151–7. https://doi.org/10.1016/j.copbio.2018.01.007.

[13] Hansen HG, Pristovšek N, Kildegaard HF, Lee GM. Improving the secretory capacity of Chinese hamster ovary cells by ectopic expression of effector genes: Lessons learned and future directions. Biotechnol Adv 2017;35:64–76. https://doi.org/10.1016/j.biotechadv.2016.11.008.
[14] Hansen HG, Nilsson CN, Lund AM, Kol S, Grav LM, Lundqvist M, et al. Versatile microscale screening platform for improving recombinant protein productivity in Chinese hamster ovary cells. Sci Rep 2015;5:18016. https://doi.org/10.1038/srep18016.
[15] Lewis AM, Abu-Absi NR, Borys MC, Li J. The use of 'omics technology to rationally improve industrial mammalian cell line performance. Biotechnol Bioeng 2016;113:26–38. https://doi.org/10.1002/bit.25673/abstract.
[16] Orellana CA, Marcellin E, Gray PP, Nielsen LK. Overexpression of the regulatory subunit of glutamate-cysteine ligase enhances monoclonal antibody production in CHO cells. Biotechnol Bioeng 2017;114:1825–36. https://doi.org/10.1002/bit.26316/abstract.
[17] Kuo CC, Chiang AW, Shamie I, Samoudi M, Gutierrez JM, Lewis NE. The emerging role of systems biology for engineering protein production in CHO cells. Curr Opin Biotechnol 2018;51:64–9. https://doi.org/10.1016/j.copbio.2017.11.015.
[18] Kao FT, Puck TT. Genetics of somatic mammalian cells, VII. Induction and isolation of nutritional mutants in Chinese hamster cells. PNAS 1968;60(4):1275–81. https://doi.org/10.1073/pnas.60.4.1275.
[19] Bray NL, Pimentel H, Melsted P, Pachter L. Near-optimal probabilistic RNA-seq quantification. Nat Biotechnol 2016;34:525–7. https://doi.org/10.1038/nbt.3519.
[20] Yates AD, Achuthan P, Akanni W, Allen J, Allen J, Alvarez-Jarreta J, et al. Ensembl 2020. Nucleic Acids Res 2020;48:D682–8. https://doi.org/10.1093/nar/gkz966.
[21] Love MI, Huber W, Anders S. Moderated estimation of fold change and dispersion for RNA-seq data with DESeq2. Genome Biol 2014;15:550. https://doi.org/10.1186/s13059-014-0550-8.
[22] Soneson C, Love MI, Robinson MD. Differential analyses for RNA-seq: transcript-level estimates improve gene-level inferences. F1000Research 2015;4:1521. https://doi.org/10.12688/f1000research.7563.1.
[23] Väremo L, Nielsen J, Nookaew I. Enriching the gene set analysis of genome-wide data by incorporating directionality of gene expression and combining statistical hypotheses and methods. Nucleic Acids Res 2013;41:4378–91. https://doi.org/10.1093/nar/gkt111.
[24] Subramanian A, Tamayo P, Mootha VK, Mukherjee S, Ebert BL, Gillette MA, et al. Gene set enrichment analysis: a knowledge-based approach for interpreting genome-wide expression profiles. PNAS 2005;102(43):15545–50. https://doi.org/10.1073/pnas.0506580102.
[25] Liberzon A, Subramanian A, Pinchback R, Thorvaldsdóttir H, Tamayo P, Mesirov JP. Molecular signatures database (MSigDB) 3.0. Bioinformatics 2011;27:1739–40. https://doi.org/10.1093/bioinformatics/btr260.
[26] Kanehisa M, Goto S. KEGG: kyoto encyclopedia of genes and genomes. Nucleic Acids Res 2000;28(1):27–30. https://doi.org/10.1093/nar/28.1.27.
[27] Kanehisa M, Furumichi M, Sato Y, Ishiguro-Watanabe M, Tanabe M. KEGG: Integrating viruses and cellular organisms. Nucleic Acids Res 2021;49:D545–51. https://doi.org/10.1093/nar/gkaa970.
[28] Kanehisa M. Toward understanding the origin and evolution of cellular organisms. Protein Sci 2019;28:1947–51. https://doi.org/10.1002/pro.3715.
[29] Luo W, Brouwer C. Pathview: an R/Bioconductor package for pathway-based data integration and visualization. Bioinformatics 2013;29:1830–1. https://doi.org/10.1093/bioinformatics/btt285.
[30] Manikwar P, Mulagapati SHR, Kasturirangan S, Moez K, Rainey GJ, Lobo B. Characterization of a novel bispecific antibody with improved conformational and chemical stability. J Pharm Sci 2020;109:220–32. https://doi.org/10.1016/j.xphs.2019.06.025.
[31] Galluzzi L, Pietrocola F, Levine B, Kroemer G. Metabolic control of autophagy. Cell 2014;159:1263–76. https://doi.org/10.1016/j.cell.2014.11.006.
[32] Kaur J, Debnath J. Autophagy at the crossroads of catabolism and anabolism. Nat Rev Mol Cell Biol 2015;16:461–72. https://doi.org/10.1038/nrm4024.
[33] Boada-Romero E, Letek M, Fleischer A, Pallauf K, Ramón-Barros C, Pimentel-Muiños FX. TMEM59 defines a novel ATG16L1-binding motif that promotes local activation of LC3. EMBO J 2013;32:566–82. https://doi.org/10.1038/emboj.2013.8.
[34] Nishimiya D, Mano T, Miyadai K, Yoshida H, Takahashi T. Overexpression of CHOP alone and in combination with chaperones is effective in improving antibody production in mammalian cells. Appl Microbiol Biotechnol 2013;97:2531–9. https://doi.org/10.1007/s00253-012-4365-9.
[35] Borth N, Mattanovich D, Kunert R, Katinger H. Effect of increased expression of protein disulfide isomerase and heavy chain binding protein on antibody secretion in a recombinant CHO cell line. Biotechnol Prog 2005;21:106–11. https://doi.org/10.1021/bp0498241.
[36] Hussain H, Maldonado-Agurto R, Dickson AJ. The endoplasmic reticulum and unfolded protein response in the control of mammalian recombinant protein production. Biotechnol Lett 2014;36:1581–93. https://doi.org/10.1007/s10529-014-1537-y.
[37] Dorners AJ, Wasley LC, Kaufman RJ. Increased synthesis of secreted proteins induces expression of glucose-regulated proteins in butyrate-treated Chinese hamster ovary cells. J Biol Chem 1989;264(34):20602–7. https://doi.org/10.1016/S0021-9258(19)47105-6.
[38] Pobre KFR, Poet GJ, Hendershot LM. The endoplasmic reticulum (ER) chaperone B. JBC 2019;294:2098–108. https://doi.org/10.1074/jbc.REV118.002804.
[39] Ho SCL, Wang T, Song Z, Yang Y. IgG aggregation mechanism for CHO cell lines expressing excess heavy chains. Mol Biotechnol 2015;57:625–34. https://doi.org/10.1007/s12033-015-9852-7.
[40] Brown AJ, Sweeney B, Mainwaring DO, James DC. Synthetic promoters for CHO cell engineering. Biotechnol Bioeng 2014;111:1638–47. https://doi.org/10.1002/bit.25227/abstract.
[41] Estes B, Hsu YR, Tam LT, Sheng J, Stevens J, Haldankar R. Uncovering methods for the prevention of protein aggregation and improvement of product quality in a transient expression system. Biotechnol Prog 2015;31:258–67. https://doi.org/10.1002/btpr.2021.
[42] Gomez N, Barkhordarian H, Lull J, Huh J, GhattyVenkataKrishna P, Zhang X. Perfusion CHO cell culture applied to lower aggregation and increase volumetric productivity for a bispecific recombinant protein. J Biotechnol 2019;304:70–7. https://doi.org/10.1016/j.jbiotec.2019.08.001.
[43] Lamark T, Johansen T. Aggrephagy: selective disposal of protein aggregates by macroautophagy. Int J Cell Biol 2012:736905–21. https://doi.org/10.1155/2012/736905.
[44] He CL, Bian YY, Xue Y, Liu ZX, Zhou KQ, Yao CF, et al. Pyruvate kinase M2 activates mTORC1 by phosphorylating AKT1S1. Sci Rep 2016;6:21524. https://doi.org/10.1038/srep21524.
[45] Xiong Q, Li W, Li P, Yang M, Wu C, Eichinger L. The role of ATG16 in autophagy and the ubiquitin proteasome system. Cells 2018;8:2. https://doi.org/10.3390/cells8010002.